

The correlation function of radio sources

A. J. Loan,¹ J. V. Wall² and O. Lahav,¹

¹ *Institute of Astronomy, Madingley Road, Cambridge, CB3 0HA*

² *Royal Greenwich Observatory, Madingley Road, Cambridge, CB3 0EZ*

Received ; accepted , 1996

ABSTRACT

We investigate the large-scale clustering of radio sources in the Green Bank and Parkes-MIT-NRAO 4.85 GHz surveys by measuring the angular two-point correlation function $w(\theta)$. Excluding contaminated areas, the two surveys together cover 70 per cent of the whole sky. We find both surveys to be reasonably complete above 50 mJy. On the basis of previous studies, the radio sources are galaxies and radio-loud quasars lying at redshifts up to $z \sim 4$, with a median redshift $z \sim 1$. This provides the opportunity to probe large-scale structures in a volume far larger than that within the reach of present optical and infrared surveys. We detect a clustering signal $w(\theta) \approx 0.01$ for $\theta = 1^\circ$. By assuming an evolving power-law spatial correlation function in comoving coordinates $\xi(r_c, z) = (r_c/r_0)^{-\gamma} (1+z)^{\gamma-(3+\epsilon)}$, where $\gamma = 1.8$, and the redshift distribution $N(z)$ of the radio galaxies, we constrain the r_0 - ϵ parameter space. For ‘stable clustering’ ($\epsilon = 0$), we find the correlation length $r_0 \approx 18 h^{-1}$ Mpc, larger than the value for nearby normal galaxies and comparable to the cluster-cluster correlation length.

Key words: galaxies: clustering – radio galaxies – large-scale structure

1 INTRODUCTION

Surveys of galaxies selected by their optical or infrared emission reveal the rich structure of the universe. This clustering structure can be quantified by using statistical techniques, such as the two-point correlation function in two (e.g. APM: Maddox et al. 1990) or three (e.g. IRAS: Fisher et al. 1993) dimensions. However, these surveys only probe the local universe: for example, the median redshift of the APM survey is $z \sim 0.1$. In contrast, radio galaxies and radio-loud quasars can be detected over significant cosmological distances, up to redshifts $z \sim 4$. However, such bright sources of radio emission represent a small fraction of all galaxies, sampling the large volume within which they can be observed much more sparsely than normal galaxies.

The prevailing consensus has long held that the distribution of radio galaxies is almost isotropic, with any structures barely detectable. Webster (1976) studied the distribution of over 7500 sources from 3 separate radio surveys at 148 MHz, 408 MHz and 1.4 GHz, concluding that the data were consistent with a uniform random distribution to within a few per cent. Shaver & Pierre (1989) demonstrated that the distribution of nearby ($z < 0.02$) radio galaxies was flattened towards the Supergalactic Plane. More recently, Peacock & Nicholson (1991) analyzed a redshift survey of 300 nearby ($z < 0.1$) radio galaxies, measuring a power-law spatial correlation function with a correlation length $r_0 = 11.0 \pm 1.2 h^{-1}$ Mpc, much larger than that for optically-

selected galaxies ($r_0 \sim 5 h^{-1}$ Mpc – Peebles 1980). Benn & Wall (1995) showed how the apparent isotropy of radio sources may be used to estimate the largest scales of cellular structure; further background and references are given therein.

The clustering of radio sources in the 4.85 GHz Green Bank survey of the northern hemisphere (87GB: Gregory & Condon 1991) has been studied recently, making use of the angular two-point correlation function $w(\theta)$ (Kooiman, Burns & Klypin 1995; Sicotte 1995). Both of these studies find that there is clearly detectable clustering signal in the 87GB survey. A preliminary correlation function analysis of the first ~ 15 per cent of the FIRST survey also finds significant clustering of radio sources (Cress et al. 1996).

This paper presents a new study of the large-scale structures traced by the radio sources in the 87GB survey. We also present a correlation function analysis of the Parkes-MIT-NRAO survey (PMN: Griffith & Wright 1993). The PMN survey used much the same method as the 87GB survey to produce a complementary 4.85 GHz survey covering most of the southern sky. With appropriate selection of angular coverage and flux-density limit, the two surveys prove to be quite well matched, covering most of the celestial sphere. Nevertheless, we analyze the surveys separately to avoid any problems arising from small systematic differences in source detection procedure and flux-density limit.

In Section 2 we examine the 87GB and PMN surveys to demonstrate their suitability for correlation function analy-

arXiv:astro-ph/9612190v1 19 Dec 1996

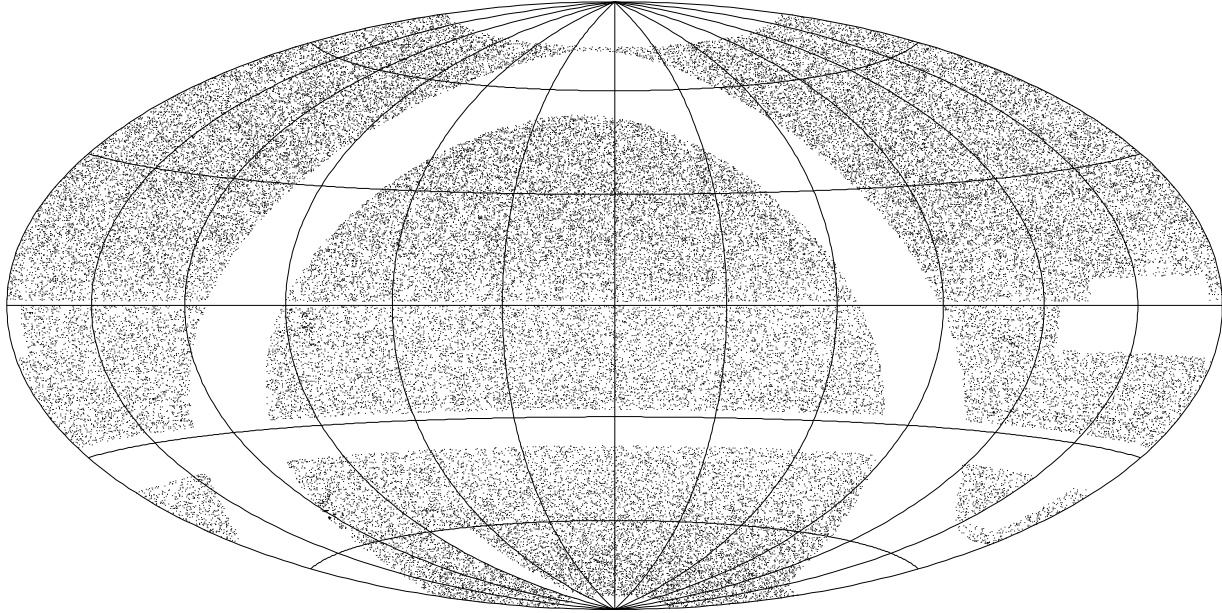


Figure 1. The 87GB (northern hemisphere) and PMN (southern hemisphere) source catalogues in Equatorial coordinates, Aitoff projection. The Galactic Plane ($|b| < 10^\circ$) and areas of poor coverage or confusion (see Table 1) have been excised. The varying source density reflects the declination dependence of the flux limits of 87GB and PMN, quantified in Figure 2.

sis. In Section 3 we present the results of our analysis, while Section 4 outlines the formalism that we use to estimate the parameters of the correlation function in three dimensions. In Section 5 we discuss the implications of our results and compare them to those of other studies.

2 THE RADIO CATALOGUES

2.1 The Green Bank survey (87GB)

The 87GB source catalogue was compiled by Gregory & Condon (1991) from observations taken in 1987 October by Condon, Broderick & Seielstad (1989) using a seven-beam receiver attached to the (now defunct) NRAO 300 foot (91 m) radio telescope in Green Bank, West Virginia, USA. The telescope was tracked back and forth along the local meridian at $\pm 10^\circ \text{ min}^{-1}$, the diurnal rotation of the earth eventually providing a Nyquist spacing of a half beam-width between adjacent observations. The data were reduced automatically using a $5\text{-}\sigma$ source-detection criterion to produce a catalogue of 54,579 sources covering the declination band ($0^\circ < \delta < +75^\circ$) for all right ascensions, except for four small confused or noisy areas. The 87GB survey has a total sky coverage of ~ 6.0 steradians.

2.2 The Parkes-MIT-NRAO survey (PMN)

The PMN source catalogue was compiled from observations taken in 1990 June and 1990 November with the ANRAO 64 m radio telescope in Parkes, NSW, Australia, covering the declination range $-87.5^\circ < \delta < +10.0^\circ$ for all right ascensions. These observations followed the same observing

Table 1. Areas from the 87GB and PMN surveys included in and excluded from our analysis.

Included:	
87GB:	$75^\circ > \delta > 1^\circ$
PMN:	$0^\circ > \delta > -28^\circ$
	$-38^\circ > \delta > -85^\circ$
Excluded:	
Galactic Plane:	$ b < 10^\circ$
Solar interference:	$6^\circ > \delta > 1^\circ$ and $ \alpha - 205^\circ < 20^\circ$
Extended sources:	$\delta < -60^\circ$ and $ \alpha - 80^\circ < 10^\circ$
	$\delta > -10^\circ$ and $ \alpha - 205^\circ < 30^\circ$
	$-30^\circ > \delta > -50^\circ$ and $ \alpha - 200^\circ < 10^\circ$

procedure using the same seven-beam receiver, and were reduced using an algorithm similar to that used with 87GB. However, a slightly different source-detection criterion was adopted: 90 per cent reliability – equivalent to $\sim 4.4\text{-}\sigma$ – rather than a $5\text{-}\sigma$.

The source catalogue was split into 4 zones according to the elevation of the telescope (see Table 1 of Wright et al. 1994): Southern, Tropical, Equatorial and Zenith (respectively: Wright et al. 1994; Griffith et al. 1994; Griffith et al. 1995; Wright et al. 1996). However, because the Parkes telescope tracks very slowly in the 10° wide region near the local zenith, the data from the Zenith zone were observed using a different strategy to the other three zones and is of a much lower quality. For these reasons, the Zenith zone is excluded from our analysis, leaving the other three zones which together cover an total area of ~ 6.4 steradians.

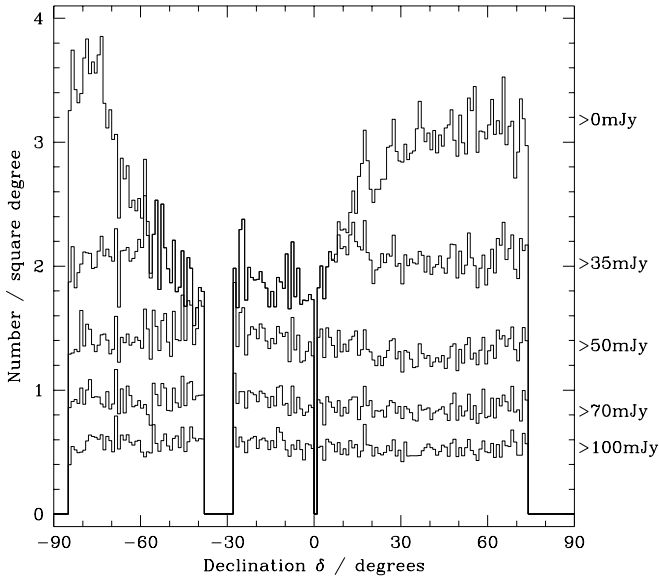


Figure 2. Histogram of the surface density of radio sources in the 87GB ($\delta > 1^\circ$) and PMN ($\delta < 0^\circ$) source catalogues as a function of declination, for a range of flux-density limits (35, 50, 70 and 100 mJy).

2.3 Comparing the 87GB and PMN surveys

Before the 87GB and PMN source catalogues can be used for correlation function analysis, we need to show that they are well matched, with no large gradients caused by instrumental or other systematic effects. We note that real large-scale structures, such as the Supergalactic Plane, will introduce inhomogeneities in these catalogues on large angular scales. We will address this issue elsewhere (Baleisis et al. 1996) but here assume that real large-scale structures appear on small angular scales and use whole-sky uniformity as our criterion for completeness.

The 87GB and PMN surveys overlap in the declination band $0^\circ < \delta < 10^\circ$ (≈ 0.59 steradians). Griffith et al. (1995) examined this overlap region, finding agreement within the quoted errors between both the published flux densities and the positions of the sources. However, both Griffith et al. (1995) and Baleisis (1996) report a worrying 2 per cent difference between the flux calibration of the 87GB and PMN catalogues, in the sense that sources in the PMN survey are assigned a systematically lower flux density than those in the 87GB survey. For this reason, and to highlight any discrepant results, we treat the surveys separately. We note that such a small calibration offset will not significantly affect the results of our analysis on small scales, as we discuss below.

The flux-density limit of the 87GB survey varies with declination, increasing from ~ 25 mJy at high declinations ($\delta > 60^\circ$) to ~ 40 mJy at the equator (Gregory & Condon 1991), for two main reasons. First, there is an elevation dependence of the sensitivity of the 300 foot Green Bank telescope, and secondly, adjacent observing tracks become increasingly further apart at lower declinations. The Parkes

telescope does not suffer from the problem of decreased sensitivity at low elevations. However, the increased coverage due to adjacent scans lying closer together at far-southern declinations ($\delta < -70^\circ$) causes the flux-density limit to decrease from ~ 50 mJy near the local zenith ($\delta \sim -33^\circ$) to ~ 40 mJy near the southern equatorial pole.

We use 87GB in the northern hemisphere ($\delta > 1^\circ$) because 87GB has a flux limit which is lower than that for PMN over the region of overlap. We discard the region within 10° of the Galactic Plane to avoid contamination by Galactic radio sources, and we also discard the area where there is solar interference in the 87GB survey, together with three areas with confusion from extended sources in the PMN catalogue. The discarded areas are shown in Table 1.

The remaining sources, shown in Figure 1, form the catalogue which we use in our correlation analysis. Figure 1 still shows a strong variation in source density with declination due to changes in the local flux-density limit. To counteract this effect, we must impose a higher flux limit over both surveys.

We plot the surface density of radio sources in the 87GB and PMN catalogues as a function of declination in Figure 2 for flux-density limits of 35, 50, 70 and 100 mJy in order to find a safe lower flux-density limit, which will provide a source catalogue with uniform sensitivity across the whole area. Both surveys are largely incomplete at the 35 mJy flux limits, with large density gradients caused by the sensitivity problems discussed above. The surface density of sources becomes increasingly more uniform as the limit is raised from 50 mJy, through 70 mJy to 100 mJy. Above 50 mJy, the surveys appear to be sufficiently evenly matched over the whole sky to allow structure on small angular scales to be studied using correlation techniques. We will also calculate correlation functions at a limit below 50 mJy to demonstrate the effect of variable sensitivity on the measured clustering.

There remains some suggestion of larger-scale structure present in the combined 87GB/PMN source catalogue which we examine elsewhere (Baleisis et al. 1996).

3 THE ANGULAR CORRELATION FUNCTION

The two-point correlation function is a measure of how clustered the sources are compared to a random Poisson distribution (e.g. Peebles 1980). The angular two-point correlation function $w(\theta)$ gives the excess probability of finding two sources in the solid angles $\delta\Omega_1$ and $\delta\Omega_2$ separated by an angle θ . One way to estimate this function (Hamilton 1993) is to compare the distribution of real galaxies to the distribution of points in a random catalogue with the same boundaries, that is:

$$w(\theta) = \frac{DD \cdot RR}{(DR)^2} - 1 \quad (1)$$

where DD , RR and DR are the numbers of data-data, random-random and data-random pairs separated by the distance $\theta + \delta\theta$. The estimation of RR and DR requires a catalogue of ‘objects’ scattered uniformly over an area with the same selection properties as the data catalogue (i.e. with the same angular boundaries). The number of ‘objects’ in the random catalogue may be very much greater than that

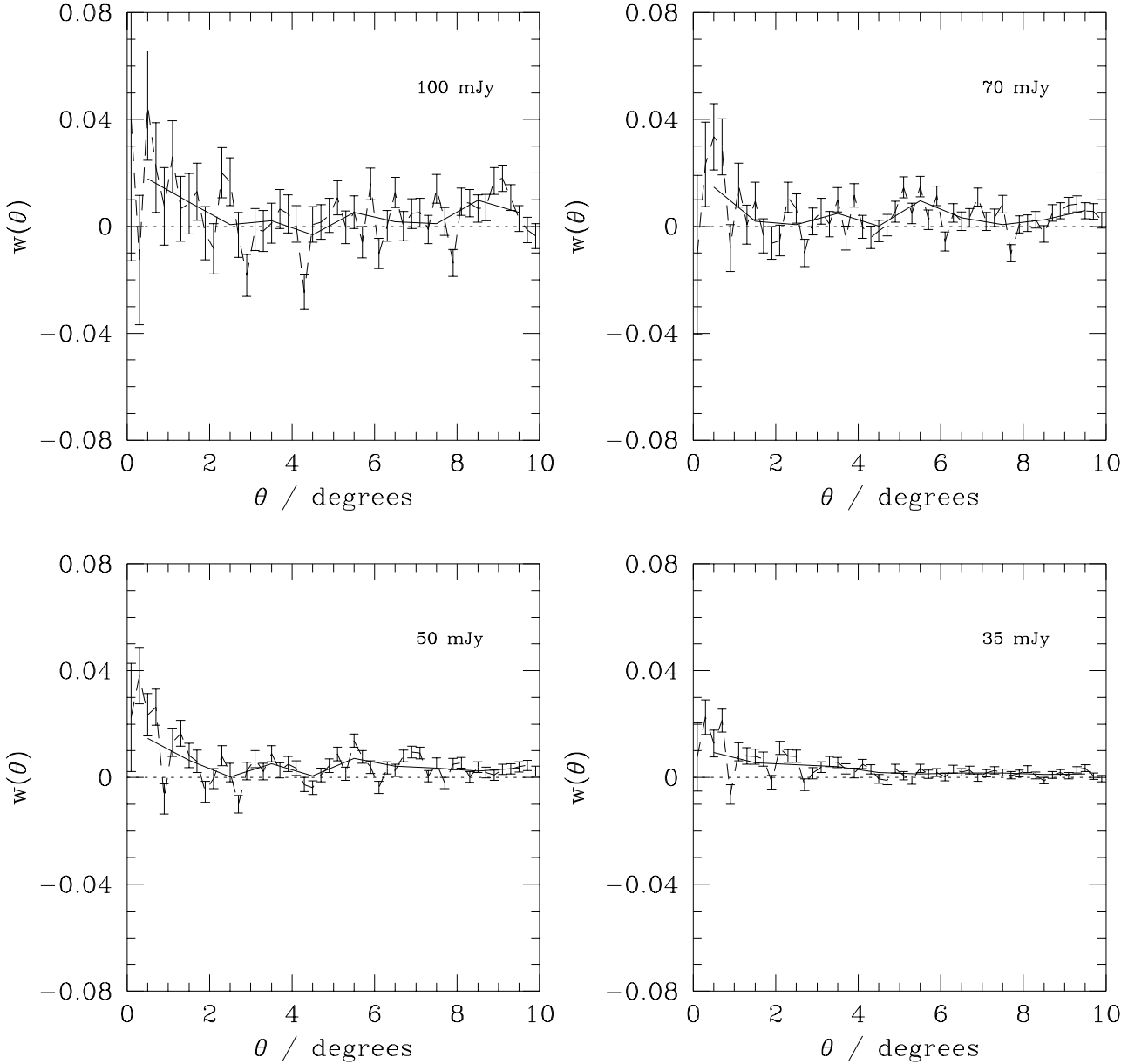


Figure 3. Angular correlation function $w(\theta)$ for the 87GB survey, with flux-density limits of 100 mJy, 70 mJy, 50 mJy and 35 mJy. In each case the dashed line shows the data in 0.2° bins, and the solid line in 1° bins. Poisson error bars are shown on the line for 0.2° bins. The excess positive signal at small angles ($\theta < 2^\circ$) increases in amplitude at higher flux-density limits.

in the real catalogues to reduce the errors in the estimates of DR and RR .

We have calculated the angular two-point correlation functions for the 87GB and PMN surveys separately, to highlight any discrepant results and also to avoid problems if the catalogues prove to be mismatches. The calculated correlation functions for the 87GB and PMN catalogues are shown in Figure 3 and Figure 4, respectively. These figures show an excess positive signal (i.e. $w(\theta) > 0$) at small angles ($\theta < 2^\circ$) with increasing amplitude at higher flux limits. This increased amplitude arises from the ‘washing out’

of structures by foreground or background sources in surveys with a lower flux-density limit. A shallower survey is expected to show a higher amplitude of the correlation function since this ‘washing out’ is less severe. However, a survey with a higher flux-density limits contains fewer sources, leading to larger errors in the estimate of $w(\theta)$ which may conceal the greater expected amplitude.

The correlation function for the 35 mJy-limit PMN catalogue, fourth panel of Figure 4, shows the effect of large-scale density gradients in the survey noted from Figure 2. These gradients are caused by choosing sources at a flux-

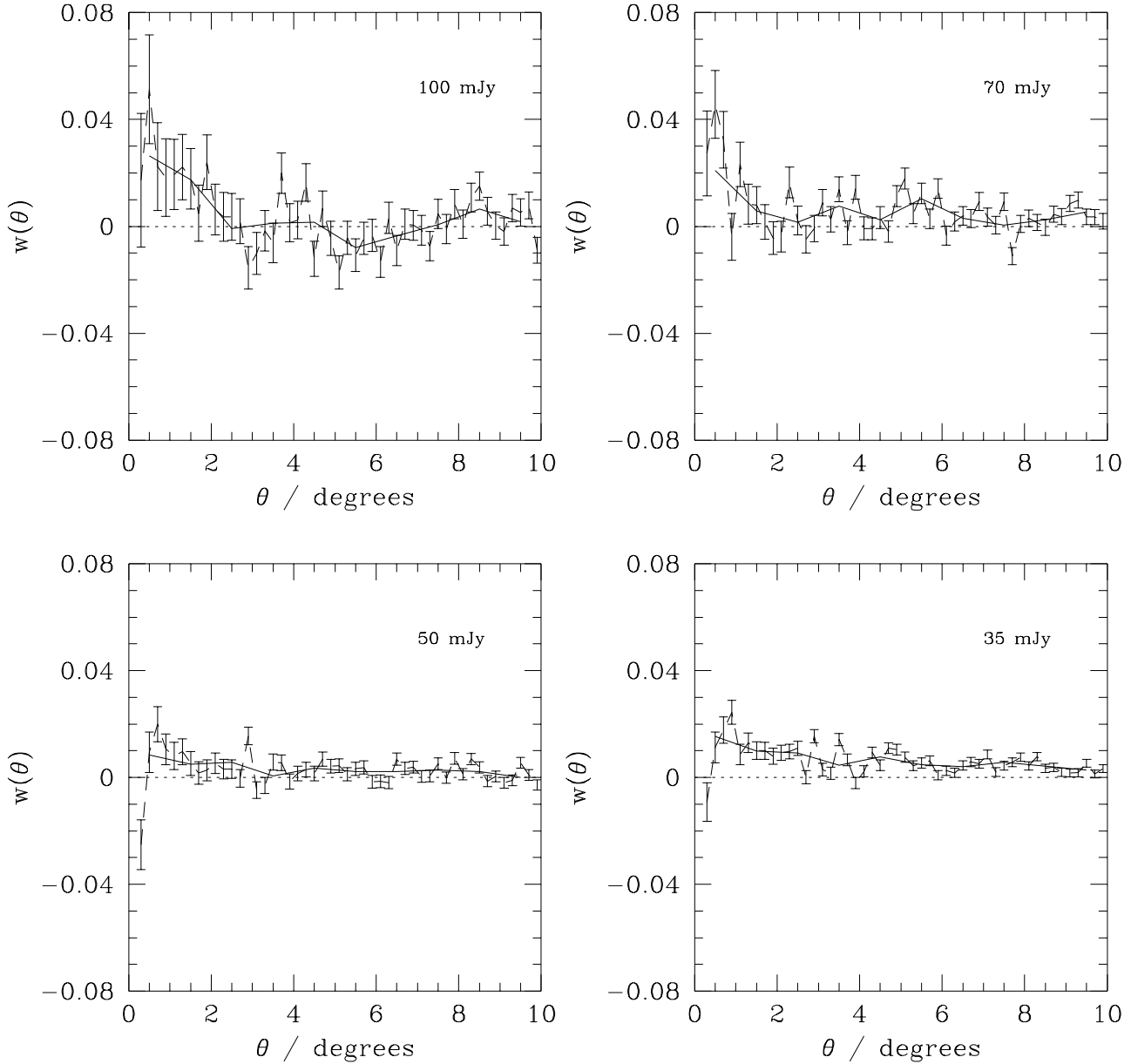


Figure 4. Angular correlation function $w(\theta)$ for the PMN survey, for flux-density limits of 100 mJy, 70 mJy, 50 mJy and 35 mJy. In each case the dashed line represents 0.2° bins and the solid line 1° bins. Poisson error bars are shown for the 0.2° binning. There is excess positive signal at small angles ($\theta < 2^\circ$); the 35 mJy plot shows the effect of the large density gradients below a flux-density completeness limit.

density limit below that of the catalogue completeness, producing a large error in the measured correlation function.

We assume the usual power-law form for the angular correlation function, such that

$$w(\theta) = A\theta^{1-\gamma}. \quad (2)$$

If we assume $\gamma = 1.8$, as found for local galaxies (Peebles 1980), then only the amplitude A of $w(\theta)$ remains to be estimated from our measurements. We have estimated this

amplitude by a simple least-squares procedure, by summing over the i bins of our calculated correlation function:

$$A_{\text{est}} = \frac{\sum_i w_i \theta_i^{1-\gamma}}{\sum_i \theta_i^{2-2\gamma}}, \quad (3)$$

where w_i is the observed value of $w(\theta)$ in the bin at angular separation θ_i . Note that different bins of the observed $w(\theta)$ are correlated. Figure 5 shows our estimates for the amplitude of the correlation function for various binning schemes

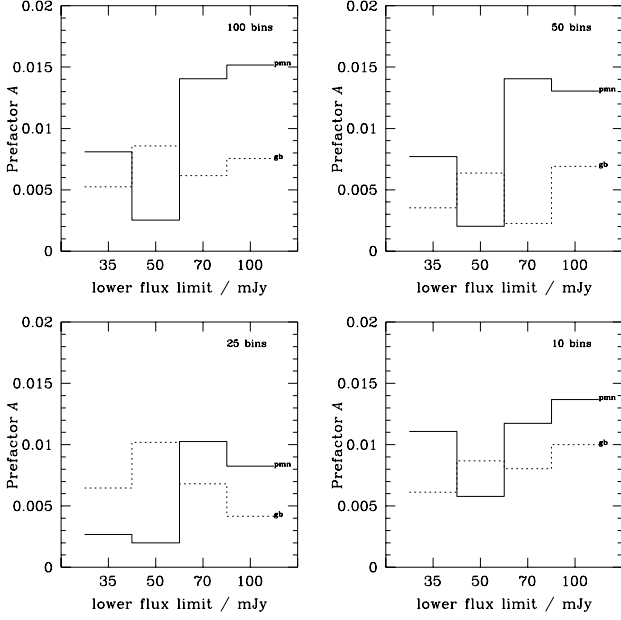


Figure 5. Estimated correlation function amplitude A in the expression $w(\theta) = A\theta^{1-\gamma}$ for a variety of different binnings, for each chosen flux-density limit. 87GB is shown with a dashed line, PMN with a solid line. The lowest flux-density limit, 35 mJy, must be regarded as suspect due to incompleteness. The remaining suggest a systematic trend with higher amplitude at higher flux limit.

and flux limits. Our estimates indicate that the amplitude A has a value between 0.005 and 0.015.

4 THE SPATIAL CORRELATION FUNCTION

4.1 The cosmological Limber's equation

Limber's equation (Limber 1953) relates the spatial correlation function $\xi(r, z)$ (in 3 dimensions) to the angular correlation function $w(\theta)$ (in 2 dimensions), given the selection function of the sample and a cosmological model. The cosmological Limber's equation can be written as (e.g. Section 56 in Peebles 1980; Baugh & Efstathiou 1993) :

$$w(\theta) = \frac{2 \int_0^\infty \int_0^\infty x^4 F^{-2} \phi^2(x) \xi(r, z) dx du}{\left[\int_0^\infty x^2 F^{-1} \phi(x) dx \right]^2}, \quad (4)$$

where x is a comoving coordinate and F takes into account the different possible world geometries (e.g. for $\Omega_0 = 1$, $\Lambda_0 = 0$, then $F = 1$). The selection function $\phi(x)$ satisfies the following relations for the mean surface density in a survey of solid angle Ω_s :

$$\mathcal{N} = \int_0^\infty x^2 \phi(x) dx = \frac{1}{\Omega_s} \int_0^\infty N(z) dz, \quad (5)$$

where $N(z) dz$ is the number of galaxies in the survey in the redshift shell $(z, z + dz)$.

Hereafter we assume a flat universe with $\Omega_0 = 1$, $F = 1$, for which the comoving distance is

$$x = \frac{2c}{H_0} [1 - (1+z)^{-1/2}], \quad (6)$$

where $H_0 = 100 h^{-1} \text{ km sec}^{-1} \text{ Mpc}^{-1}$ is the Hubble expansion parameter. We also assume a power-law redshift-dependent 3-dimensional correlation function:

$$\xi(r, z) = \left(\frac{r}{r_0} \right)^{-\gamma} (1+z)^{-(3+\epsilon)}, \quad (7)$$

where r is a proper coordinate, r_0 is the correlation scale length at redshift $z = 0$, and ϵ describes the redshift evolution of the spatial correlation function. In comoving coordinates, this can be written as:

$$\xi(r_c, z) = \left(\frac{r_c}{r_0} \right)^{-\gamma} (1+z)^{\gamma-(3+\epsilon)}, \quad (8)$$

where $r_c = r(1+z)$ is a comoving coordinate. Specific values of ϵ can be interpreted as follows: $\epsilon = 0$ corresponds to constant clustering in proper coordinates, i.e. 'stable clustering'; $\epsilon = \gamma - 3 = -1.2$ implies constant clustering in comoving coordinates; $\epsilon = \gamma - 1 = 0.8$ implies growth of clustering under linear theory (e.g. Peebles 1980; Treyer & Lahav 1996).

For our purpose it is more convenient to express Limber's equation in term of $N(z)$. Using Equation 5 and Equation 6 we can write:

$$\phi(x) = \frac{1}{\Omega_s} \frac{H_0}{c} N(z) x^{-2} (1+z)^{+3/2}. \quad (9)$$

Substituting this into Equation 4 and assuming the small angle approximation $r \approx (u^2/F^2 + x^2\theta^2)^{1/2}/(1+z)$ we find that:

$$w(\theta) = \left(\frac{r_0 H_0}{c} \right)^\gamma (2\theta)^{1-\gamma} H_\gamma \times \frac{\int_0^\infty dz \left[1 - (1+z)^{-1/2} \right]^{1-\gamma} N^2(z) (1+z)^{\gamma-\frac{3}{2}-\epsilon}}{\left[\int_0^\infty dz N(z) \right]^2}, \quad (10)$$

where $H_\gamma = \Gamma\left(\frac{1}{2}\right) \Gamma\left(\frac{\gamma-1}{2}\right) / \Gamma\left(\frac{\gamma}{2}\right)$, with Γ the Gamma function. Assuming $\gamma = 1.8$, $H_{1.8} = 3.68$.

We emphasize that these equations are only valid for a power-law correlation function of the form of Equation 7 and $\Omega_0 = 1$ universe. A more general expression is given in terms of a double integral and Fourier transforms by Baugh & Efstathiou (1993) and Treyer & Lahav (1996).

Since γ is assumed *a priori* to be 1.8, the same as that for normal galaxies, and $N(z)$ is determined from studies of the radio-source population, the only free parameters to be deduced by comparison with the observed $w(\theta)$ are the correlation scale length r_0 and the clustering evolution index ϵ . Note that the amplitude of $N(z)$ does not affect Limber's equation; only the functional form of $N(z)$ is important.

4.2 The redshift distribution $N(z)$

The prediction of the angular two-point correlation function $w(\theta)$ from the spatial correlation function $\xi(r)$ requires knowledge of the redshift distribution of the sources $N(z)$ complete to the designated flux-density limit. No complete sample of radio sources has been fully identified at the flux-density level of 50 mJy. Despite this, Dunlop & Peacock (1990) have shown how a synthesis of the statistics of radio sources (including source-counts together with incomplete identifications and measured redshifts) may be used to determine the distribution of radio sources with redshift,

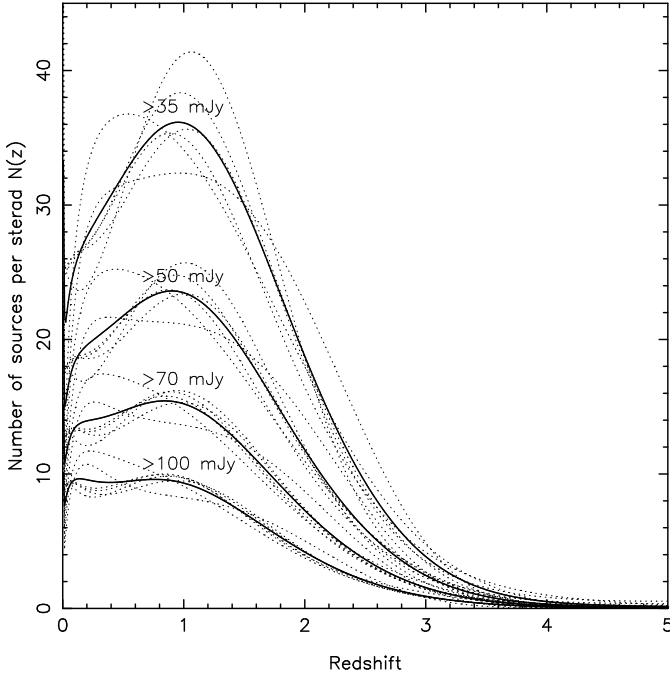


Figure 6. Redshift distributions $N(z)$ of the radio-source population selected at 4.85 GHz, shown for each flux-density limit at which $w(\theta)$ has been calculated. The solid curves represent the average of six models taken from Dunlop & Peacock (1990); see text. The dotted curves for each limit represent the 6 models from which the average was formed, indicating the uncertainty at each flux-density level due to incomplete or statistically-limited redshift data.

from which $N(z)$ may be derived at any flux density. In their analysis it was assumed that there are two independent populations of radio sources, namely the flat-(radio)spectrum and steep-spectrum objects. The former are predominantly identified with QSOs, the latter with radio galaxies; a more detailed overview of the radio-source populations is given by Wall (1994). Treating the data for flat- and steep-spectrum sources separately, Dunlop & Peacock fit polynomial expansions to describe the luminosity function and its epoch-dependence for each population. They did so from seven different starting points, the scatter amongst the seven models providing indication of the statistical definition of the space density at any point over the $P - z$ plane.

From these models we have calculated the $N(z)$ at 35, 50, 70 and 100 mJy, summing the space densities for the flat- and steep-spectrum populations. At each flux-density limit, we then take the mean from the various models as the canonical value for $N(z)$. (In this procedure we omitted model 5, which has a problem at the lower flux densities in that a dominating spike appears in the space densities and $N(z)$ close to the redshift cutoff which is specified as a starting condition for this particular formulation.) The $N(z)$ produced by this procedure is shown in Figure 6. This figure indicates that the median redshift for the radio sources in the 87GB/PMN survey is at $z \sim 1$. Figure 6 also shows that the average redshift decreases as the lower flux limit is increased.

We note that a 2 per cent flux mismatch between the catalogues has been reported (Griffith et al. 1995; Baleisis

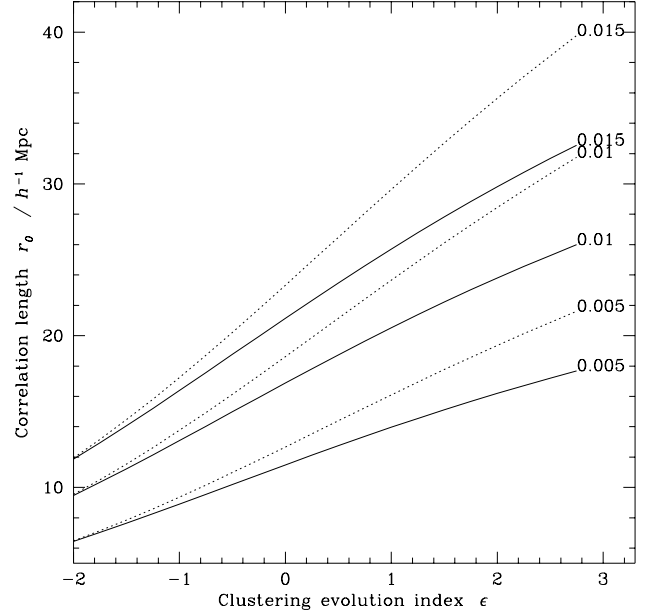


Figure 7. Predicted loci of constant A in the correlation length r_0 and clustering evolution index ϵ plane, for $S_{4.85} > 100$ mJy (solid lines) and $S_{4.85} > 50$ mJy (dotted lines). The values of r_0 and ϵ which may be deduced from a single measurement of A are strongly correlated.

1996). This mismatch would mean that the flux limits given for the correlation functions estimated above are slightly incorrect, and that we should use a different $N(z)$ corresponding to the true flux in our Limber's inversion. However, as we can see from Figure 6, the shape of $N(z)$ varies very little from one flux limit to another, and so there will be little effect on the small angular scales concerned.

4.3 Estimating the spatial correlation function

$$\xi(r, z)$$

Armed with our estimate for the amplitude of the angular correlation function from Section 3 ($A = 0.010 \pm 0.005$) and our estimate of $N(z)$ from Section 4.2, we can now compare this observed estimate to the predictions from our model of the radio galaxy population for a range of parameters, via equations 2 and 10. Figure 7 shows lines of constant $w(\theta)$ amplitude as a function of the spatial correlation length r_0 and the evolution index ϵ at a flux-density limits of 50 mJy and 100 mJy. There is a strong correlation between the values of r_0 and ϵ which can be inferred from a single measurement of A . Assuming a value for one parameter then provides an estimate for the other parameter. For example, consider $w(\theta = 1^\circ) = A = 0.01$ for a flux limit of 50 mJy. If we also assume that clustering is constant in comoving coordinates, i.e. $\epsilon = \gamma - 3 = -1.2$, then $r_0 = 13 h^{-1}$ Mpc, while if clustering is 'stable', i.e. $\epsilon = 0$, then $r_0 = 18 h^{-1}$ Mpc. The range of acceptable values of A (0.005 to 0.015) translates into a uncertainty of a few Mpc in r_0 .

5 DISCUSSION

Using two large-area 4.85 GHz radio surveys with median redshift $z \sim 1$, we have detected a correlation signal $w(\theta) \approx 0.01$ at angles $\theta \sim 1^\circ$ for radio sources brighter than 50 mJy. Adopting the best estimate of redshift distribution for the sources, we find the present-day correlation length to be in the range $13 < r_0 < 18 h^{-1}$ Mpc for evolution index in the range $-1.2 < \epsilon < 0$, with uncertainty in the measurements permitting errors as large as $\sim 5 h^{-1}$ Mpc. The values of r_0 and ϵ inferred from a measurement of $w(\theta)$ are strongly correlated.

Previous studies by Kooiman et al. (1995) and Sicotte (1995) measured angular correlation functions which were largely in agreement with each other and with our results. Kooiman et al. and Sicotte both attempted to use their results to constrain the spatial correlation function of radio galaxies, but reached contradictory results. Sicotte found good agreement between his model and his measured correlation function, with a best fit value of $\epsilon = -1$ and $r_0 = 11 h^{-1}$ Mpc. This result is in good agreement our results, even though Sicotte used an earlier (Condon 1984) and significantly different estimate of $N(z)$. (We repeated our analysis using the Condon $N(z)$ and obtained remarkably similar results; there is little sensitivity to the form of $N(z)$.) This is also in accord with the value of $r_0 = 11 h^{-1}$ Mpc measured by Peacock & Nicholson (1991) from low redshift ($z < 0.1$) radio galaxies.

On the other hand, Kooiman et al. found that the amplitude of their model was 70 times smaller than the measured correlation function, assuming $\gamma = 1.8$, $\epsilon = 0$ and $r_0 = 11 h^{-1}$ Mpc. This is clearly inconsistent with our results, and also with those of Sicotte.

Taken at face value, for a realistic range of the evolution index ϵ , we find a present-day correlation length r_0 which is far larger than that for normal optical galaxies ($r_0 \sim 5 h^{-1}$ Mpc, Peebles 1980), IRAS galaxies ($r_0 \sim 4 h^{-1}$ Mpc, Saunders, Rowan-Robinson & Lawrence 1992), and QSOs ($r_0 \sim 6 h^{-1}$ Mpc for $\epsilon = -1.2$, Shanks & Boyle 1994). However, our values of the correlation length for radio galaxies is comparable to that for clusters of galaxies ($r_0 \sim 20 h^{-1}$ Mpc, Bahcall 1988). This may reflect the preference of radio galaxies at $z > 0.5$ to reside in high-density environments (Bahcall & Chokshi 1992; Yee & Ellingson 1993 and references therein).

The uncertainty in our measurement of the correlation function could be reduced by measuring the redshifts for at least a random subset of the catalogues and cross-correlating this subset with the rest of the sample (e.g. Saunders et al. 1992). These redshifts would also improve our knowledge of the redshift distribution of the radio galaxy population $N(z)$, and indeed of the nature of the population (QSO - radio-galaxy - BL Lac object) at this flux-density level.

Our analysis demonstrates that large-scale structure studies based on new radio surveys nearing completion will provide decisive estimates of distant structure and its evolution; and we have provided the appropriate formalism. Ongoing surveys with the VLA - FIRST (Becker, White & Helfand 1995) and NVSS (Condon et al. 1996) - will yield of order 10^6 sources over the sky, thus overcoming the limitations imposed by counting errors in the estimated pair-counts from the current 4.85 GHz surveys. The first corre-

lation analysis of a subset of the FIRST survey (Cress et al. 1996) indicates that the full survey will provide strong constraints on our models of the radio source population. Furthermore, positional accuracy of these new surveys will be such that direct spectroscopy at the catalogue radio positions can be used to obtain redshifts. Knowledge of the redshifts of even a random subset of these catalogues will allow the use of cross-correlation techniques to improve the estimate of the correlation function in three-dimensions (e.g. Saunders et al. 1992).

ACKNOWLEDGMENTS

AJL acknowledges support from a PPARC studentship. We thank Audra Baleisis, Brian Boyle, Karl Fisher, Steve Maddox, and Jim Peebles for helpful discussions, and John Peacock for generously making available to us his software for calculating $N(z)$ from the Dunlop-Peacock models. The 87GB and PMN surveys are public data, generously made available to the astronomical community by the original researchers.

REFERENCES

- Bahcall N.A., 1988, ARA&A, 26, 631
- Bahcall N.A., Chokshi, A., 1992, ApJ, 382, L33
- Baleisis A., Lahav O., Loan A.J., Wall J., 1996, in preparation
- Baleisis A., 1996, M.Phil. thesis, Cambridge University
- Baugh C.M., Efstathiou G., 1993, MNRAS, 267, 323
- Benn C.R., Wall J.V., 1995, MNRAS, 272, 678
- Becker R.H., White R.L., Helfand D.J., 1995, 450, 559
- Condon J., 1984, ApJ, 287, 461
- Condon J.J., Broderick J.J., Seielstad G.A., 1989, AJ, 97, 1064
- Condon J.J., Cotton W.D., Greisen E.W., Yin Q.F., Perley R.A., Broderick J.J., 1996, AJ, in press
- Cress C.M., Helfand D.J., Becker R.H., Gregg M.D., White R.L., 1996, ApJ, in press
- Dunlop J.S., Peacock J.A., 1990, MNRAS, 247, 19
- Fisher K.B., Davis M., Strauss M.A., Yahil A., Huchra J.P., 1993, ApJ, 402, 42
- Gregory P.C., Condon J. J., 1991, ApJS, 75, 1011
- Griffith M.R., Wright A.E., 1993, AJ, 105, 1666
- Griffith M.R., Wright A.E., Burke B.F., Ekers R. D., 1994, ApJS, 90, 179
- Griffith M.R., Wright A.E., Burke B.F., Ekers R. D., 1995, ApJS, 97, 347
- Hamilton A.J., 1993, ApJ, 417, 19
- Kooiman B.L., Burns J.O., Klypin A.A., 1995, ApJ, 448, 500
- Laing R.A., Riley J.M., Longair M.S., 1983, MNRAS, 204, 151
- Limber D.N., 1953, ApJ, 117, 134
- Maddox S.J., Efstathiou G., Sutherland W.J., Loveday J., 1990, MNRAS, 242, 43P
- Peacock J.A., Nicholson D., 1991, MNRAS, 253, 307
- Peebles J., 1980, The Large-Scale Structure of the Universe, Princeton University Press, Princeton
- Saunders W., Rowan-Robinson M., Lawrence A. 1992, MNRAS, 258, 134
- Shanks T., Boyle B.J., 1994, MNRAS, 271, 753
- Shaver P.A., Pierre M., 1989, A&A, 220, 3
- Sicotte H., 1995, Ph.D. thesis, Princeton University
- Treyer M.A., Lahav O., 1996, MNRAS, 280, 469
- Wall J.V., 1994, Austr. J. Phys., 47, 625
- Webster A., 1976, MNRAS, 175, 61

- Wright A.E., Griffith M.R., Burke B.F., Ekers R.D., 1994, ApJS, 91, 111
Wright A.E., Griffith M.R., Hunt A.J., Troup E., Burke B.F., Ekers R.D., 1996, ApJS, 103, 145
Yee H.K.C., Ellingson E., 1993, ApJ, 411,43